Symbol Synchronizer Assembly Instability Study: Part II

R. C. Bunce
Network Operations Office

Part I (Ref. 1) developed a simple frequency ramp model to initiate understanding of the Symbol Synchronizer Assembly (SSA) instability at low bit rates in narrow bandwidths. Part II, presented here, describes extensive data processing to develop a third-order phase model and then to translate all such processed data to the frequency realm for further analysis. The frequency study yields a long frequency modulation (FM) drift sinusoid (1600-s period), an impressed secondary drift wave with a period of about 116 s, and a set of even harmonics of twice the ramp period—the latter arising from, and used to modify, the phase detector model. The result is applied secondarily to estimate the strong-signal SSA phase detector response "out-of-lock." Finally, the main drift components are verified against all available data, and the result is used to estimate minimum lock conditions and the SSA drift effect under normal operating modes. The instability problem appears marginally resolvable if the acquisition technique is modified.

I. Spurious Drift Model Phase Reduction

An SSA simplified block diagram is shown in Fig. 1, with several parameters of the study noted. The loop phase error, point ①, affects the time pulses at point ②. The integrator varies in synchronization with the input symbol stream by this error. The output, absoluted and combined with additive system noise, is then sampled over 30-s periods. The samples are appropriately combined in a common algorithm to yield sequential estimates of S/N in dB (point ③).

The S/N data in this study varied widely, indicating that the phase error was passing through all possible values, and the loop was continually going "in- and out-of-lock," if the idea of "lock" applies at all under such conditions.

In order to study the phase error at point ①, from the data at point ③, and finally isolate the spurious phase behavior at the VCO output, point ②, it was necessary to perform several data reduction steps (see Table 1):

(1) The effect of absoluting the S/N computation input, and the addition of system noise at this point, must be removed. A very complicated algorithm due to Lesh (Ref. 1) yielded a curve that was empirically fit over the lower region after sys-

tem noise was removed by simple variance subtraction. The system noise, designated DBY, was estimated from the maximum S/N seen (+26 dB) during very-strong-signal runs.

(2) The modified S/N, now approximately linear with signal, was reduced to phase equivalent and fit with a third-order polynomial across a subject out-of-lock ("ramp") data region. This fit gave an approximate function for use in the S/N computation model.

(3) Since the phase varied across the sampling period, the phase equivalent and the true "central" phase during S/N computation differed.

Also, phase jitter and the phase variance across the sampling period appeared as additional noise, when the loop had no phase control. After some trial, the jitter effect was removed by simply dropping the input S/N (from 18 to 17.3 dB) and computing, then simply adding, the variance of the deterministic phase function within the period.

After all of the above effects were enacted, the resulting S/N was reduced to central phase estimates and compared with the original phase at (2) above. The differences were fit to a third-order curve designed to cancel the summation displacement effect, and the difference rms was evaluated. The process was iterated until the rms was below 1 deg. The final modified phase data (10 points) were considered to estimate the actual phase at central time of the S/N sampling period.

In order to find spurious drift accurately, it was necessary to remove loop "internal" effects due to phase detector response in the out-of-lock region. This response was simply modeled as a cosine wave with half-period of the ramp duration; the model was a rough approximation to common strong-signal analysis curves (see Table 2). The modified phase data were (again) fit to a third-order function, and this function became the argument for the phase detector model. The model was singly numerically integrated for the first-order filter effect and doubly numerically integrated for the second-order filter effect. The resulting sum phase was subtracted from the data phase and the process iterated until parameters stabilized. This yielded phase data substantially free of internal effects and a deterministic function expressing the residual model. This was the same point reached in Part I (Ref. 1), except that the data were "clean" and the spurious drift model was third-order. The process would not have been fully valid, except that the S/N sampling period vastly increases S/N; the residual rms is less than 1.0 deg.

Investigation of the model immediately showed the value of the third-order term. In all trials, the second- and third-order term signs *opposed* one another, indicating a peak frequency near the center of the ramp period. Also, the second-order term was much smaller (0.8×10^{-6} vs. 4.4×10^{-6} Hz/s) than in Part I. These effects led to the conclusion that the data should be investigated in the frequency realm; the function was being masked by phase consideration only.

II. Spurious Drift Frequency Analysis

The final phase data from above, roughly free of all expected effects, were differenced analytically to obtain a frequency data set. They consisted of an obviously complicated waveform (about 0.5×10^{-3} Hz P-P) with a large offset (1.5×10^{-3} Hz) and a small negative ramp, as above. A program was established to process a "growing" FM model and compute differences and rms at each stage; semiautomated variation of parameter techniques were used (see Table 3):

(1) The offset and ramp were estimated and removed. A predominant apparent sinusoid with a period of 116 s was the residual.

(2) The sinusoid was estimated (amplitude and phase) and added.

(3) Residuals with periods of about 240 and 60 s appeared, roughly 20 dB down. They were estimated and added.

(4) The "raw" frequency of all available data (23 points) covering 1100 s was plotted. It showed a predominant "1 + cosine" waveform with a period of 1600 s and an amplitude of 1.56×10^{-3} Hz P-P. The "fine" data above were just beyond the "peak"; the zero was a long lock period about 15 min earlier. This was obviously the SSA "in-lock" start point. The original "ramp" was this drift near its small-slope maximum.

(5) The main drift waveform was added, and a final component, with a period of about 480 s appeared. Also, a sharp triangle pattern of small amplitude was obvious.

(6) When all the above components were combined and parameters "trimmed," the final rms was less than 0.001×10^{-3} Hz. This is meaningless, for it lies

beyond the data resolution. The final result is shown in Fig. 2. Except for the large waveform with a 116-s period, all components other than main drift form an even harmonic series, with the fundamental that of the cosine wave phase detector model. Such a series invariably describes some combination of half-wave retification, with a "dead area." Thus, the harmonics, with some possible contribution from an indiscernible 120-s (fourth harmonic) wave, were attributed to the phase detector frequency function, the small "triangle" being the rate function residual. These were combined to yield an estimate of the phase detector function at strong signal, as shown in Fig. 3 after a single smoothing. Note the "dead area" at central period when the S/N is very small. This is possibly due to system noise effects during S/N reduction rather than being a phase detector characteristic.

Finally, it was confirmed from wideband data that the majority of the 116-s sine wave is *not* a phase detector phenomenon but rather is present as part of the drift—a secondary waveform of frequency so close to the fourth harmonic of the detector function (120-s period) that they cannot be distinguished. A check of wider-band data placed the period at the quoted 116 s.

The main ramp with this secondary component impressed is shown in Fig. 4, as noted. This result leads to the main conclusion of the analysis, that narrowband operation is limited by internal frequency drifts of the SSA. Note that all contributions in the loop except the main drift waveform lead to an rms of only 2 deg and are thus important only to describe the phase detector function.

III. Stability Criteria

The SSA stability is thus affected severely only by the main drift wave. In Part I, this was taken to be a simple frequency ramp; in this part, it has become evident as a sine wave with long period. It has a maximum rate of

$$\frac{0.76 \times 10^{-3}\, x}{800} = 3.0 \times 10^{-6}\ \text{Hz/s} \qquad (1)$$

This is some 15 times what can be simply tracked in the SSA narrow-narrow bandwidth at a data rate of 8⅓ bits/s.

However, since the disturbing drift appears to be sinusoidal *FM*, the "ramp" is of finite duration, following a sine wave pattern. Its effect can be expressed, by integration, as a phase function:

$$\phi(t) = 0.762 \int \left[1 + \cos\left(\frac{\pi}{800} t + \alpha\right)\right] dt + \phi_0$$

$$= 0.762t + \frac{0.762 \times 800}{\pi} \sin\left(\frac{\pi}{800} t + \alpha\right) + \phi_0$$

$$\phi(t)\ \text{deg} = 0.762 \times 360 \times 10^{-3} t + \frac{0.762 \times 800}{\pi}$$

$$\times 360 \times 10^{-3} \sin\left(\frac{\pi}{800} t + \alpha\right) + \phi_0$$

or

$$\phi(t)\ \text{deg} = 0.273t + 69.3 \sin\left(\frac{2\pi}{1600} t + \alpha\right) + \phi_0$$

$$\approx 7.0 \times 10^{-7} t^3 \text{ at acquisition} \qquad (2)$$

This expression is quite significant. The frequency of the second term (1/1600 Hz) is below any tracking bandwidth in the SSA, and will be attenuated, or "tracked out," at least partially, under all operating conditions. In the narrow-bandwidth and 8⅓-bit/s condition, it is attenuated to an amplitude of only 19.5 deg rms, or marginally *within tracking range*; even the transient overshoot can possibly be handled. However, the leading term is present because acquisition takes place (zero frequency) at the negative extreme of the wave. This term, like a frequency step, cannot be "zeroed," or tracked with the sine wave present. A change in acquisition technique could possibly relieve this. Note the cubic approximation at present acquisition.

If acquisition "zero" took place at the wave midpoint, overshoot would only be to about 27 deg, and the frequency offset would be missing. Automated acquisition at the low-frequency extreme of the wave is the final basis for the instability behavior.

The secondary term leads to

$$\phi(t) = 0.279 \int \cos\left[\frac{\pi}{58} t + \alpha_1\right] + \phi_1$$

$$\phi(t)\ \text{deg} = \frac{0.279 \times 58 \times 360 \times 10^{-3}}{\pi} \sin\left(\frac{\pi}{58} t + \alpha_1\right) + \phi_1\ \text{deg}$$

$$= 1.90\ \text{deg} \sin\left(\frac{\pi}{58} t + \alpha_1\right) + \phi_1\ \text{deg}$$

The frequency of this term is 0.0083 Hz, indicating prominence in the narrow-medium bandwidth, 8⅓-bit/s

configuration. The term is small but leads to variations of about 0.5 dB. Such variations were observed at a frequency with a period of about 116 s. As noted, this confirmed that the "fourth harmonic" was a true spurious component and not a phase detector harmonic.

Both the above components are small—"tracked-out"—in larger bandwidths. The larger component is less than 1.0 deg peak (0.13 dB) when the bandwidth is increased 4:1, to 0.00668 Hz. The secondary component becomes indistinguishable at all bandwidths above this.

The analytical expressions used in all the above descriptions are summarized, as noted, in Tables 1 through 3.

IV. Summary

Part I (Ref. 1) indicated the presence of a phase ramp rate (frequency drift) beyond narrowband tracking capability, but data only marginally conclusive. Part II investigated the S/N ratio data from the SSA for a number of phase and frequency effects: pre-absoluting, summation-period phase displacement, loop internal contributions, and finally, spurious frequency drift. The data were adjusted to remove all but the spurious products by data processing of out-of-lock points, translated to frequency using several iteration procedures. Both the strong-signal phase detector function and the drift process were modeled, and the phase detector function was determined and sketched.

The spurious frequency drift model showed that the "ramp" of Part I was actually part of an FM sinusoid pair consisting of two components, a large one with a period of 1600 s and a secondary one with a period of about 116 s. Both presumably arose from the SSA search oscillator. The magnitude was compatible with manufacturers' specifications.

Phase functions of the frequency sinusoids were determined and analyzed. They have little effect above a bandwidth of 0.01 Hz but are important below this point. An approximate 0.5-dB jitter occurs at narrow-medium 8⅓ mode due to the secondary component, and lock is not possible in narrow-narrow 8⅓ mode, under present conditions, due to the major drift component offset.

Thus, the major conclusion of the entire study, Part I and Part II, is that a large FM internal drift is present (about 25-min period), together with a secondary FM drift (about 116-s period), and these drifts cannot presently be tracked in SSA bandwidths narrower than 0.01 Hz. Such bandwidths occur only in the narrowband SSA configuration. Even in this configuration, it appears that lock could be marginally held with the present drift if "in-lock" and oscillator-stop were declared in the "middle" of the drift cycle, when the oscillator ramp was greatest. This is not, however, the present mechanization.

References

1. Bunce, R. C., "Symbol Synchronization Assembly Instability Study: Part I," in *The Deep Space Network Progress Report 42-28*, pp. 95–105, Jet Propulsion Laboratory, Pasadena, Calif., Aug. 15, 1975.
2. Lesh, J. R., "Accuracy of the Signal-to-Noise Ratio Estimator," in *The Deep Space Network Progress Report*, Technical Report 32-1526, Vol. 10, pp. 217–235, Jet Propulsion Laboratory, Pasadena, Calif., Aug. 15, 1972.

Table 1. SSA S/N conversion to linear phase data

Step	Expressions	Definitions and notes
System noise removal	$DB_{1_i} = -10 \log [10^{-(DBS_i/10)} - 10^{-(DBY/10)}]$	DBS_i = S/N data at T_i DBY = system S/N = 26 dB
Absolute correction (empirical fit)	$DBL_i = \begin{cases} DB_{1_i} & DB_{1_i} > 5 \\ DB_{1_i} + \left[1 - \dfrac{6}{DB_{1_i} + 1}\right] & DB_{1_i} < 5 \end{cases}$	DBX = signal S/N = 17.3 dB in ramp
Initial phase estimate	$\hat{\phi}_{1_i} = \dfrac{K}{2} \pm \dfrac{1}{4} \{1 - 10^{[(DBL_i - DBX)/20]}\}$, cycles	$K = 0$, SIGN = + : $\hat{\phi}_{1_i} < 1/4$ $K = 1$, SIGN = − : $\hat{\phi}_{1_i} > 1/4$ single ramp only
Correction for S/N central phase offset	$\hat{\phi}_{N_i} = a_{0_N} + a_{1_N}(\hat{\phi}_{1_i}) + a_{2_N}(\hat{\phi}_{1_i})^2 + a_{3_N}(\hat{\phi}_{1_i})^3$	
Continuous phase function estimate	$\hat{\phi}_N(t) = b_{0_N} + b_{1_N} \cdot t + b_{2_N} \cdot t^2 + b_{3_N} \cdot t^3$	N = iteration index S = normalized signal level
S/N algorithm model (linearized by above reduction steps)	$\hat{R}_{N_i} = \dfrac{\bar{S}^2}{2\sigma_S^2}$ $\quad \bar{S} = \dfrac{1}{31} \sum_{n=-15}^{15} [1 - 4\hat{\phi}_N(T_i)]$ $\sigma_S^2 = \dfrac{1}{R^*} = \dfrac{1}{31} \sum_{n=-15}^{15} [1 - 4\hat{\phi}_N(T_i) - \bar{S}]^2$	R^* = DBX converted to power ratio $a_{0_N}, a_{1_N}, a_{2_N}, a_{3_N}$ yielded by least-squares fit of set $\phi_{1_i}, \hat{\phi}_{N_i}'$ $b_{0_N}, b_{1_N}, b_{2_N}, b_{3_N}$ yielded by least-squares fit of set $T_i, \hat{\phi}_{N_i}$
Phase differential computation and iteration	$\hat{\phi}_{N_i}' = \dfrac{K}{2} \pm \dfrac{1}{4}\left[1 - \dfrac{\hat{R}_{N_i}}{R^*}\right]$ yields the a_n with ϕ_{1_i} set $\phi_{E_i} = (\hat{\phi}_{N_i} - \phi_1)$ if $\sigma_{\phi_E} < 1$ deg, iteration stopped	

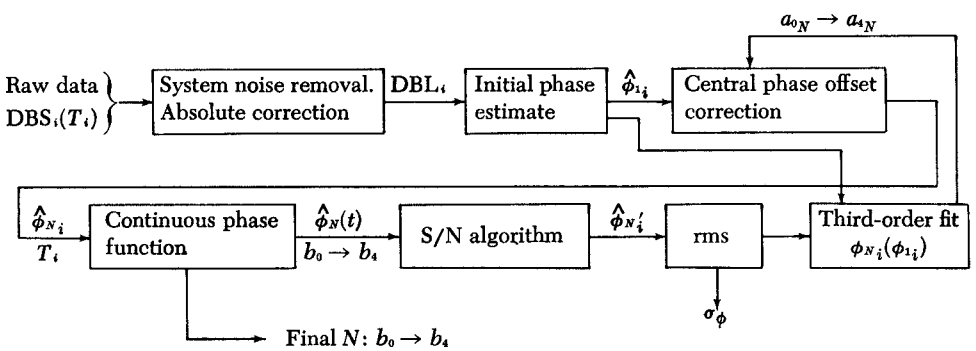

Table 2. Out-of-lock phase detector initial model

Step	Expressions	Definitions and notes
Initial empirical phase detector model	$\hat{V}(\phi) = V_{max} \cos\left[2\pi \cdot \frac{4}{3} \cdot \left(\phi - \frac{1}{16}\right)\right]$	V = phase detector output voltage $\frac{4}{3}$ and $-\frac{1}{16}$
First-order phase term	$\dot{\phi}(V_{max}) = -2W\Delta\phi_{max} = -\frac{W}{8}$	Confine ½-cycle to ramp period
	$\hat{\phi}_{I1_i} = -\frac{W}{8}\int_0^{T_i} \cos\left\{\frac{8\pi}{3}\left[\hat{\phi}_N(t) - \frac{1}{16}\right]\right\} dt$	W = loop bandwidth at $G \approx 2G_0$; $\zeta = 1$
Second-order phase term	$\ddot{\phi}(V_{max}) = -W^2\Delta\phi_{max} = -\frac{W^2}{16}$	Integration numerically by machine
	$\hat{\phi}_{I2_i} = -\frac{W^2}{16}\int_0^{T_i}\int_0^{\tau} \cos\left\{\frac{8\pi}{3}\left[\hat{\phi}_N(t) - \frac{1}{16}\right]\right\} dt\, d\tau$	$W = 0.00129$ Hz $W \cdot TS = 0.000155$
Phase correction	$\hat{\phi}_{IN_i}(t_i) = \hat{\phi}_{I1_i} + \hat{\phi}_{I2_i}$ $\hat{\phi}_{N_i} = (\hat{\phi}_{N-1_i} - \hat{\phi}_{IN_i})$ $\hat{\phi}_N(t) = b_{0_N} + b_{1_N}t + b_{2_N}t^2 + b_{3_N}t^3$	$TS = \frac{1}{8\frac{1}{3}} = 0.120$ (strong signal)
	Iteration stopped when parameters stabilize to 1×10^{-4}.	
Final parameter values for out-of-lock set chosen	$b_0 = 0.06252$ cycles $= 22.51$ deg $b_1(0) = 0.94862$ mHz $2b_2(0) = 8.065\ \mu$Hz/s $6b_3(0) = -0.0559806\ \mu$Hz/s^2	

Table 3. Frequency conversion and analysis

Step	Expressions	Definitions and notes
Phase to frequency conversion estimate	$F_i(T_i) = \frac{1}{2}\left[\frac{\phi_i - \phi_{i-1}}{T_i - T_{i-1}} + \frac{\phi_{i+1} - \phi_i}{T_{i+1} - T_i}\right]$	$F_R(t)$ = residual after estimating $F_N(t)$
Component analysis	$F_{N_i}(T_i) = \sum_{n-1}^{N-1} F_N(T_i) - F_i(T_i)$ $E_{N_i} = A_N \begin{Bmatrix}\sin\\ \cos\end{Bmatrix}(2\pi f_N T_i + a_N) - F_{N_i}(T_i)$ σ_{E_N} minimized by variation of parameters A_N, f_N, a_N after observational estimates.	One small component showed a triangular, rather than sinusoidal, form. It was apparently the phase detector model F residual, as noted.
Final equation ($\sigma_{EN} < 10^{-4}F$) F, mHz $F_0 = 0.00209059$ Hz (period = 478.334 s)	$F(t) = 0.761658\left[1 + \cos\left(\frac{2\pi}{1600}t + 0.12\right)\right]$ $+ 0.003$ $- 0.2788 \cos\left[\frac{2\pi}{117.2}t + 0.133603\right]$ (secondary drift) $+ 0.064 \sin(2\pi \cdot F_0 t + 0.1956)$ $- 0.052 \sin(2\pi \cdot 2F_0 t + 0.24886$ $+ F(4F_0 t)$ {could not be distinguished from secondary drift} $+ 0.038665 \cos(2\pi \cdot 8F_0 t + 0.0)$ } phase detector model components (see text) $- \begin{cases} 0.002 - 0.000123t & t < 100 \\ 0.04216 + 0.000273t & t > 100 \end{cases}$ model $\dot{f}$ residual	

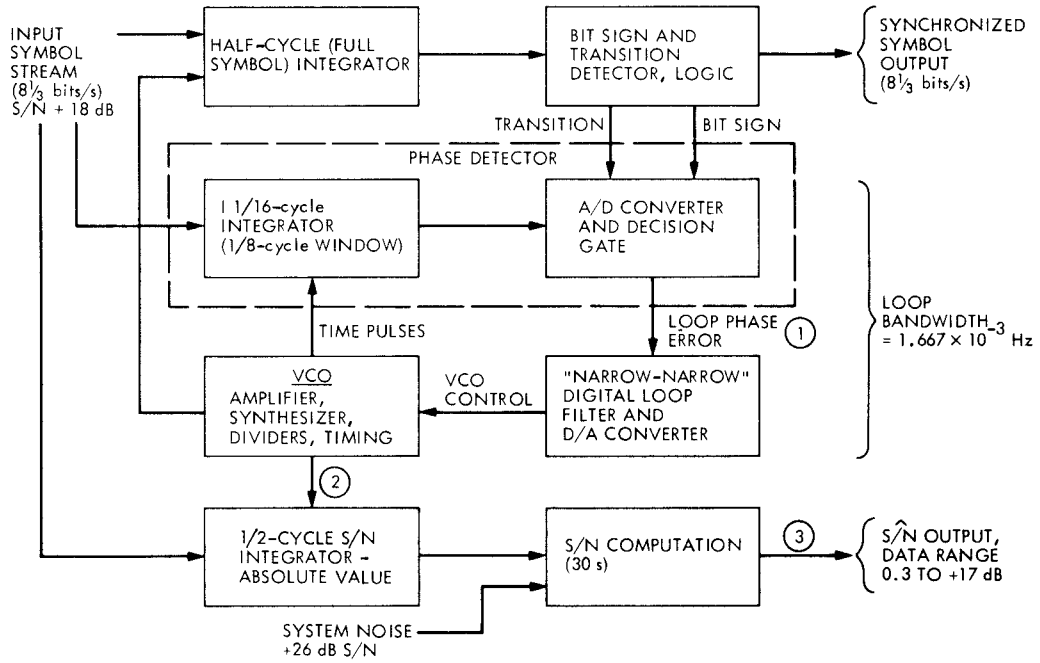

Fig. 1. SSA simplified block diagram with values noted while data were taken

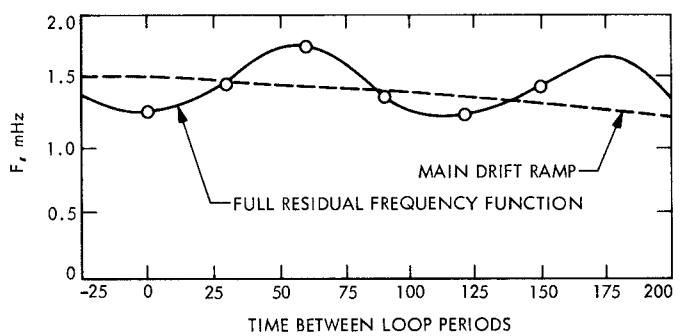

Fig. 2. SSA phase detector mean strong-signal characteristic (+18 dB S/N), as reconstructed from harmonic analysis of frequency data

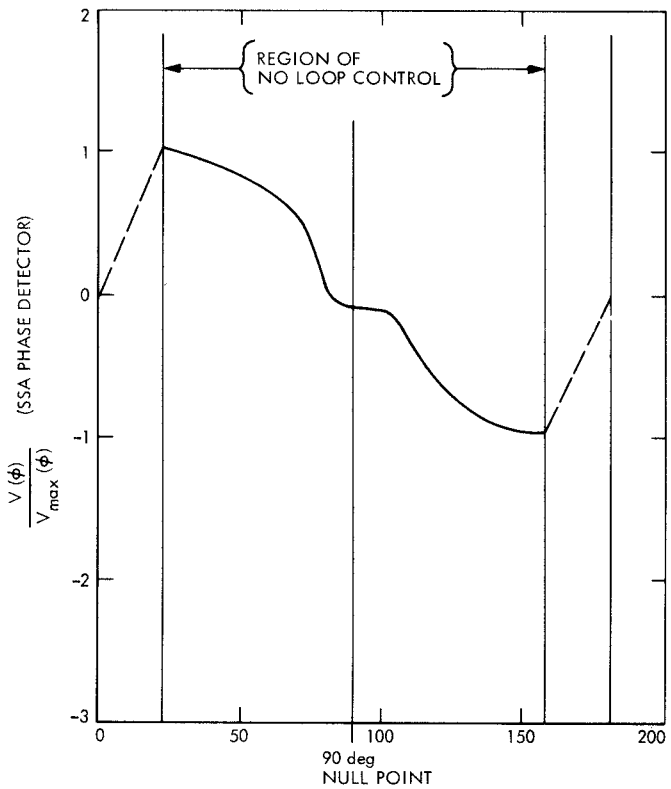

NOTE:

"DEAD AREA" NEAR 90 deg PROBABLY THE RESULT OF SYSTEM-NOISE-LIMITING RESIDUAL SIGNAL DURING S/N REDUCTION RATHER THAN A TRUE PHASE DETECTOR CHARACTERISTIC

Fig. 3. Main drift and secondary wave adjusted for estimated fit to extended "raw" data

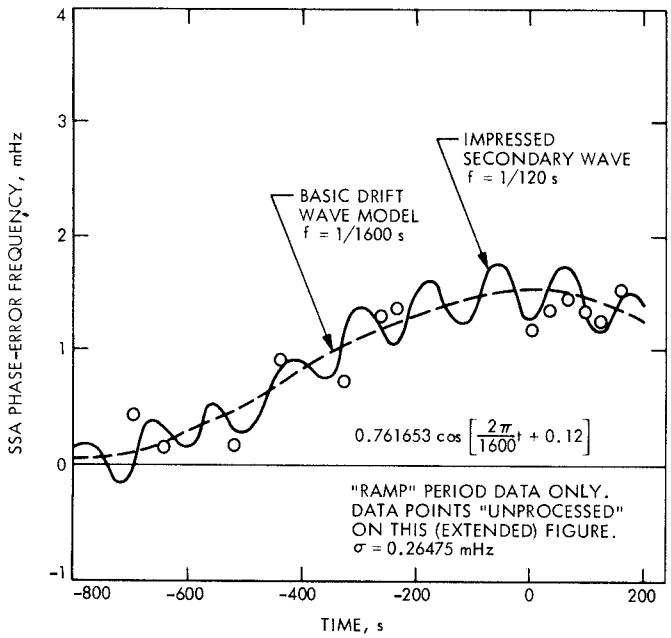

Fig. 4. Residual frequency function obtained by processing pre-adjusted phase data from SSA S/N output, narrow-narrow 8⅓-bit/s mode